

Experimental investigation of novel pre-tightened teeth connection technique for composite tube

Fei Li ^{1a}, Qilin Zhao ^{*2}, Haosen Chen ^{3b} and Longxing Xu ^{4c}

¹ Institute of Logistics Engineering of PLA, Chongqing 400000, China

² School of Mechanical and Power Engineering, Nanjing University of Technology, Nanjing 210007, China

³ Institute of Advanced Structure Technology, Beijing Institute of Technology, Beijing 100081, China

⁴ The First Research Division, General Equipment Department of the PLA, Wuxi 214035, China

(Received April 26, 2016, Revised December 14, 2016, Accepted December 15, 2016)

Abstract. A new composite tube connection method called the pre-tightened teeth connection technique is proposed to improve the composite tube connection efficiency. This paper first introduces the manufacturing process of the proposed technique. It then outlines how the mechanical properties of this technology were tested using four test groups. The factors that influence the load-bearing capacity and damage model of the connection were analyzed, and finally, the transfer load mechanism was investigated. The following conclusions can be obtained from the research results. (1) The new technique improves the compressive connection efficiency by a maximum of 79%, with the efficiency exceeding that of adhesive connections of the same thickness. (2) Changing the depth of teeth results in two types of damage: local compressive damage and shear damage. The bearing capacity can be improved by increasing the depth, length, and number of teeth as well as the pre-tightening force. (3) The capacity of the technique to transfer high loads is a result of both the relatively high interlaminar shear strength of the pultruded composite and the interlaminar shear strength increase provided by the pre-tightening force. The proposed technique shows favorable mechanical properties, and therefore, it can be extensively applied in the engineering field.

Keywords: composite tube; pre-tightened teeth connection; connection efficiency; influence factors

1. Introduction

Composite tubes are widely used in civil engineering because they are light in weight, have high strength, and show good corrosion resistance (Prachasaree *et al.* 2009, Li *et al.* 2005). However, compared to steel tubes, which have been widely used in space grid structures and space trusses (Huang *et al.* 2015), applications of composite tubes are currently limited to structures with a low load capacity and low span. This is because of the high initial investment, imperfect manufacturing techniques, complicated design calculation theory, and, more importantly, the lack of efficient connection techniques (Ju *et al.* 2011).

To date, the main connection techniques employed for composite components are bolt, adhesive, and bolt-adhesive hybrid connections (Starikov and Schön 2001, Oh 2007, Li *et al.* 2010). Bolt connections can be applied to join composite components with different cross sections. However, the hole-forming process destroys the fiber continuity and leads to higher stress concentrations, which affect the load capacities of connections (Karakuzu *et al.* 2008, Scarselli *et al.* 2015). Bolt connections of composites

are particularly susceptible to shear damage because of the single alignment of fiber (Rosales-Iriarte *et al.* 2011, Girão Coelho *et al.* 2015). Adhesive connections provide a smooth non-destructive joining technique for two dissimilar materials (Ucsnik *et al.* 2010). Different physical characteristics such as the influence of the overlap length, joint-end configurations, fiber orientation of the composites, and surface preparation have been investigated in detail (Kinloch 1994). Bolt-adhesive hybrid techniques combine the use of adhesives and bolts. Thicker glue layers and a modified fabrication technique can improve the load capacity of bolt connections (Esmaeili *et al.* 2014, Gamdania *et al.* 2015). The bolt and bolt-adhesive hybrid methods are mainly applied in the composite plane. Composite tubes are typically joined using adhesives. Numerous studies have focused on this type of connection. Stress analyses of smart composite pipe joints integrated with piezoelectric composite layers under torsional loading have been conducted (Cheng and Li 2008). An analytical model was developed for tubular adhesive bonded joints based on the application of the variational principle for the potential energy of deformation occurring in adhesive layers (Nemes *et al.* 2006). To determine the effect of the overlap length on the torsional capacity of tubular adhesive bonded joints, a finite element investigation was conducted by Hosseinzadeh and Taheri (2009). A finite difference solution for the stress analyses of tubular adhesive bonded joints subjected to torsional loading was introduced by Wei and Li (2010). This connection does not weaken structures,

*Corresponding author, Professor,
E-mail: lifei609@163.com

^a Ph.D., E-mail: 939093519@qq.com

^b Ph.D., Professor, E-mail: chspla@163.com

^c Ph.D., Student, E-mail: 939093519@qq.com

and a cover tube connection concentrates the shearing and peel stresses at the connected ends, which limits the load transferring capacity (Das and Pradhan 2014). In addition, adhesive connections cannot be used to join composite tubes in different orientations.

In this study, a new composite tube connection method called the pre-tightened teeth connection (PTTC) technique was developed. This paper describes this connection technique for composite tubes in detail, and main factors influencing the efficiency of the technique and load transfer mechanism were experimentally analyzed. The findings demonstrate that this connection method capitalizes on the advantages of the composite tube. Furthermore, this joint technique can be used to join composite tubes in different orientations using bolted or welded connections for the metal components.

2. Structure of PTTC

The PTTC consists of an external metal tube, middle composite tube, and internal metal tube. Ring-shaped teeth are manufactured at the connecting end of the composite tube, with well-matched teeth on the metal piece connected to the composite (Fig. 1). The external load is transferred via the shear stress of the bottom layer of the composite teeth and the friction force at the connecting surface. Moreover, the end of the composite tube is supported by an internal metal tube. This can prevent the composite tube from being damaged when a certain radial stress is exerted on the composite teeth. The composite tube can be connected to the external metal via bolt or weld connections (Fig. 2).

The pre-tightening force exerted on the composite is an

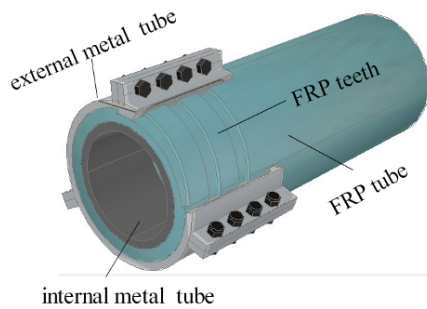


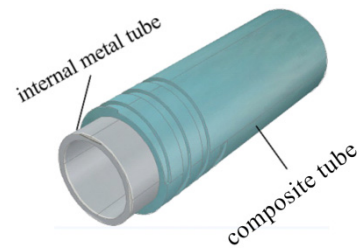
Fig. 1 Illustration of composite tube connection



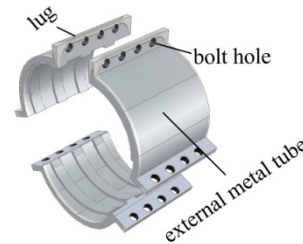
Fig. 2 Composite tube connection based on PTTC

important factor in the high bearing capacity of the connection. The pre-tightening force on the composite tube can be applied in two ways.

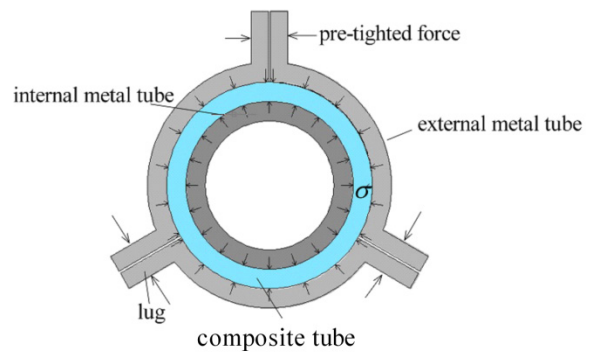
- (1) Exerting a pre-tightening force on the composite tube by stretching a circular high-strength bolt—this approach requires the following manufacturing method. First, an internal tube is manufactured, which has an outer diameter equal to the inner diameter of the composite tube. This internal metal tube is compressed into the end of the composite tube to increase the radial stiffness (Fig. 3(a)). Second, three lugs are fabricated at the external edge of the metal tube. The metal tube is then trisected at the middle of each lug, and bolt holes are drilled in each lug (Fig. 3(b)). Finally, the trisected external metal tube is installed in the composite tube. By tightening the nut with a torque wrench, a tensile stress is formed at the bolt, and a compressive stress is formed at the surface between the metal and composite tubes (Fig. 3(c)).
- (2) Exerting a pre-tightening force on the composite tube by interference fit—the internal metal tube, the outer diameter of which is larger than the inner diameter of the composite tube, is compressed into



(a) Internal metal tube compressed into composite tube



(b) Fabricated external metal tube



(c) External metal tube installed in composite tube

Fig. 3 Illustration of pre-tightening force exerted by bolt

the composite tube. A compressive stress forms at the surface between the metal and composite tubes. The manufacturing process is as follows: an external metal tube with internal spiral teeth (without lugs) and a composite tube with external spiral teeth are prefabricated. The metal tube is installed in the composite tube via rotation (Fig. 4(a)). An internal metal tube, whose outer diameter is larger than the inner diameter of the composite one, is then fabricated. The amount of interferential fit is calculated according to the magnitude of the pre-tightening force (Fig. 4(b)). Finally, the internal metal tube is compressed into the composite tube via a pressure device (Fig. 4(c)). This approach generates the pre-tightening interface force by pressing the internal metal tube into the composite tube.

Each method of exerting the pre-tightening force has advantages. The magnitude of the pre-tightening force can be arbitrarily adjusted, and the pre-tightening force can also be adjusted during the connection process by stretching the circular high-strength bolt. However, lugs and high-strength bolts are needed, which increases the weight and cost of this joint. If the pre-tightening force is exerted via an inter-

ferential fit, no additional facility for the external metal tube are required, which can effectively reduce the weight of the joint, but the pre-tightening force cannot be adjusted.

3. Experimental procedures

To study the connection properties and factors that influence the bearing capacity of the composite tube PTTC, four groups with different lengths, depths, pre-tightening forces, and number of teeth were studied. The damage process for the joint could not be observed because the composite tube PTTC was wrapped by an external metal tube. However, composite plate teeth connections could be simply fabricated, and the deformations of these structures were easily observed during experiments. Although a composite plate and composite tube have geometric differences, the stress distributions in their shear planes are the same (Deng *et al.* 2013). Thus, the factors that influence the bearing capacity of a composite tube PTTC could be obtained based on the factors that influence the bearing capacity of the composite plate PTTC. In this study, composite plates were manufactured for two test groups in order to research the effects of the length and width of teeth on the connection property. Furthermore, the joint damage process was observed, and the strain field at the critical location was measured. Based on the composite pre-tightened teeth plate connection, two test groups were designed for the composite tube in order to research the influence of the pre-tightening force and number of teeth on the bearing capacity. The connection efficiency was analyzed in the experiment using various numbers of teeth.

3.1 Materials

- (1) Bolt: an A2-70 high-strength bolt was used, which had a diameter, compressive strength, and yield strength of 6 mm, 700 MPa, and 450 MPa, respectively.
- (2) Composite: pultruded glass fiber composite plates and tubes were used in the experiment, with the fiber direction generally 0° . The fiber fraction was approximately 50% by weight, of which approximately 89.15% was glass fiber and 10.85% was combined mats. The compressive strength of the material in the fiber direction was 560 MPa.
- (3) Metal: Q345 steel was used, which had a yield strength of 235 MPa.

The detailed material parameters are listed in Table 1.

3.2 Specimen configuration

The pre-tightened teeth composite plate was manufactured as follows: composite and steel plates with the same width were first selected, and symmetric teeth were fabricated on these using a milling machine. Second, bolt holes were drilled into the composite tooth space and at the corresponding positions on the steel plate. Finally, bolts were installed in the bolt holes, and a torque wrench was used to apply 30 Nm of torque to each bolt. The normal stress was exerted on the composite plate by applying a pre-

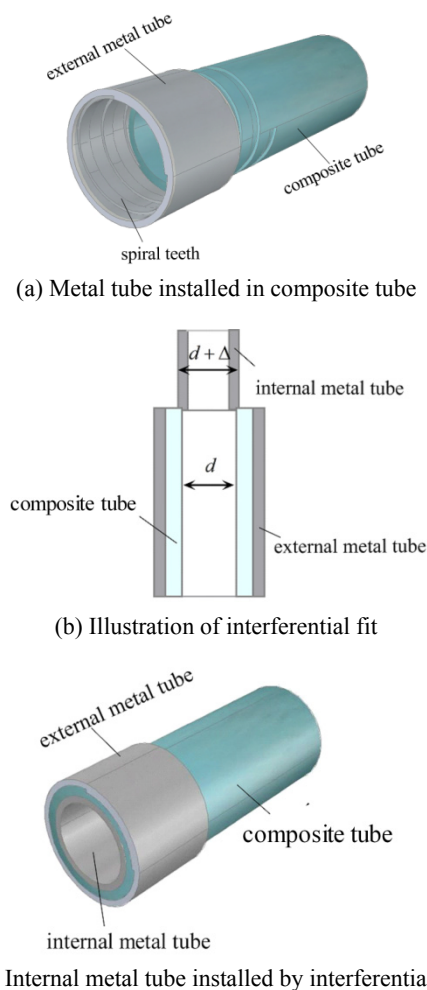


Fig. 4 Illustration of pre-tightening force exerted by interferential fit

Table 1 Material parameters

Material	E_x GPa	E_y GPa	E_z GPa	ν_{xy}	ν_{yz}	ν_{xz}	G_{xy} GPa	G_{yz} GPa	G_{xz} GPa
Composite	30	8	8	0.32	0.32	0.34	5.4	3.5	5.4
Steel	2e5	2e5	2e5	0.3	0.3	0.3	113	113	113

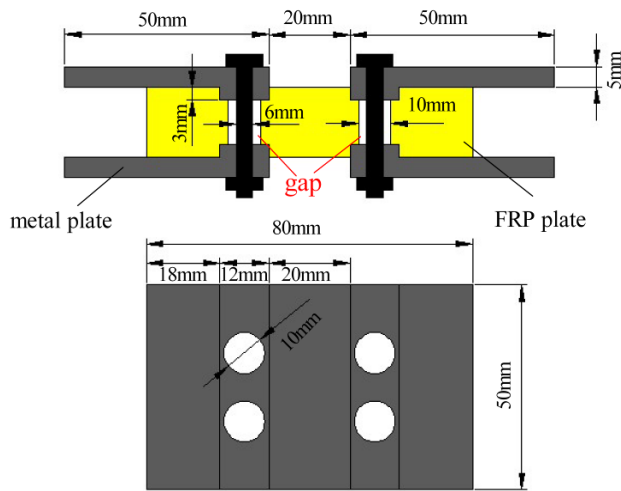


Fig. 5 Geometry of composite plate pre-tightening force tooth connection

tightening force to the high-stress bolt in the bolt hole, as shown in Fig. 5.

Two test groups were designed to examine the effects of the depth and length of teeth; the composite plate width and thickness were 50 mm and 17 mm, respectively. The bolts were not supposed to transfer the load, and the diameter of the bolt hole (10 mm) had to exceed the diameter of the bolt (6 mm) for the load transfer process (Fig. 5). In the first test group, the teeth were 25 mm long, and the composite teeth were 0.5 mm, 1 mm, 1.5 mm, 2 mm, and 4 mm deep. Two specimens were prepared according to the different depths of teeth (Table 2). In the second test group, the teeth were 2 mm deep, and the composite teeth were 9 mm, 12 mm, 23 mm, 25 mm, and 30 mm long. Two specimens were prepared according to the different lengths of teeth (Table 2).

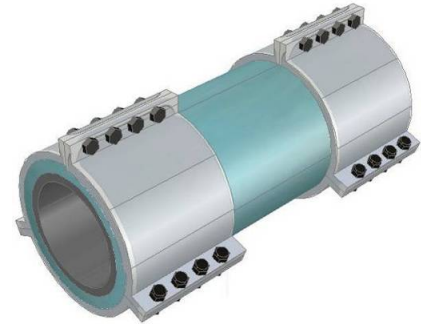
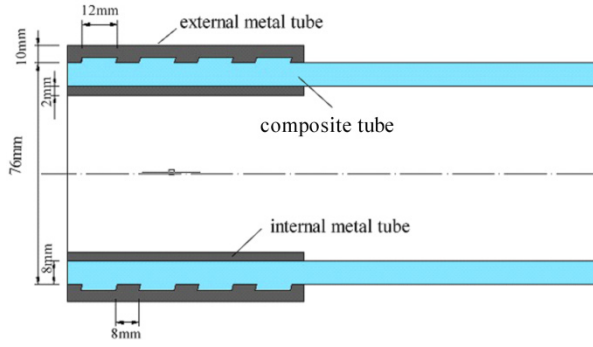
Two groups were designed to examine the effects of the number of teeth and pre-tightening force; the diameter and thickness of the composite tube were 76 mm and 17 mm, respectively. The pre-tightening force was exerted by stretching the circular high-strength bolt. The number of teeth was varied in the first test group. The length of the teeth was 25 mm, the depth of the composite teeth was 2 mm, and the numbers of teeth were 1, 3, 5, 7, and 8. The corresponding bolt numbers were 1, 2, 3, 4, and 5 (Fig. 6(a)). Two specimens were prepared according to the different number of teeth (Table 3). The pre-tightening force was varied in the second test group. The length of the teeth was 12 mm, and the depth of the composite teeth was 2 mm. The number of teeth was 1, and the torques was 6, 13, 20, 30, and 56 Nm (Fig. 6(b)). Two specimens were prepared according to the different pre-tightening forces (Table 3).

Table 2 Specimen parameters

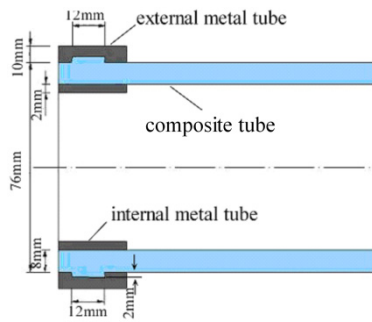
Group number	Serial number	Tooth length L_1 (mm)	Tooth depth h_1 (mm)	The pre-tight force (N.m)
1	1-P-25-0.5-1	25	0.5	30
	1-P-25-0.5-2			
	1-P-25-1-3		1	
	1-P-25-1-4			
	1-P-25-1.5-5		1.5	
	1-P-25-1.5-6			
	1-P-25-2.5-7		2	
	1-P-25-2.5-8			
	1-P-25-4-9		4	
	1-P-25-4-10			
2	2-P-9-2-1	9	2	30
	2-P-9-2-2			
	2-P-12-2-3	12		
	2-P-12-2-4			
	2-P-23-2-5	23		
	2-P-23-2-6			
	2-P-25-2-7	25		
	2-P-25-2-8			
	2-P-30-2-9	30		
	2-P-30-2-10			

3.3 Test methods and processes

A universal test machine with computer-controlled loading was utilized in the experiments, and the loading rate was 2 mm/min according to ASTM D3846-94 (Fig. 7(a)). The shear plane strains fields, loading-displacement curves, and ultimate loads for the composite plate joint were measured, and the mechanism that influenced the bearing capacity was analyzed via the measured strains. A high-speed video recorder (VW-9000) was used to capture images of the specimen (Fig. 7(b)). The obtained images were used to measure the strain field, as well as the joint damage process. Images of joints under different loads were obtained, and the image of a specimen under zero load was set as the reference image. The images of specimens under different loads were set as the target images. The strain fields under different loads were obtained using the VIC-2D software. In addition, the loading-displacement curves and ultimate loads for composite tube joints were obtained (Fig. 7(c)).



(a) Specimens with different number of teeth

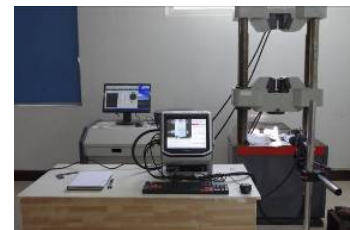


(b) Specimens with different pre-tightening forces

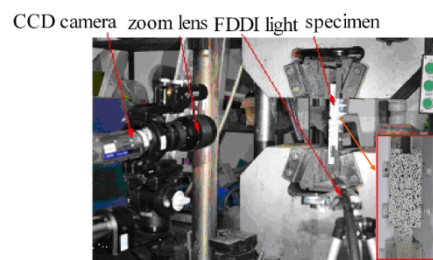
Fig. 6 Geometry of composite tube PTTC

Table 3 Specimen parameters

Group number	Serial number	Pre-tightening force (N.m)	Number of teeth	Length of teeth L_1 (mm)	Depth of teeth h_1 (mm)
3	3-S-1-6-1	6	1	12	2
	3-S-1-6-2				
	3-S-1-13-3	13			
	3-S-1-13-4				
	3-S-1-20-5	20			
	3-S-1-20-6				
	3-S-1-30-7	30			
	3-S-1-30-8				
	3-S-1-56-9	56			
	3-S-1-56-10				
4	4-S-1-56-1	56	1	12	2
	4-S-1-56-2		3		
	4-S-3-56-3		5		
	4-S-3-56-4		7		
	4-S-5-56-5		8		
	4-S-5-56-6				
	4-S-7-56-7				
	4-S-7-56-8				
	4-S-8-56-9				
	4-S-8-56-10				



(a) Experiment equipment



(b) Composite plate specimen loading



(c) Composite tube specimen loading

Fig. 7 Experiment equipment and specimen loading

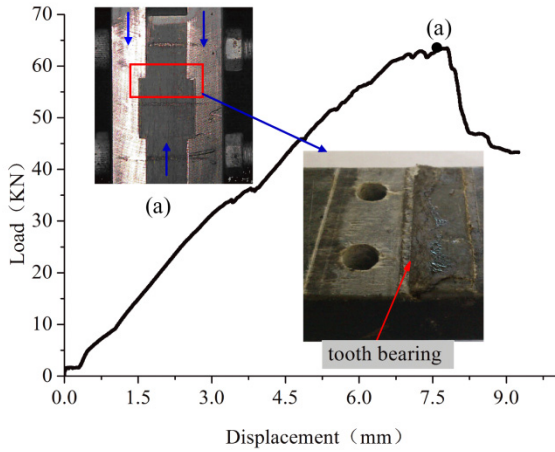


Fig. 8 Typical load–displacement curves and damage on specimen when depth of teeth is 0.5 mm

Table 4 Results of varied teeth depths

Serial number	Tooth depth (mm)	Ultimate load (kN)	Damage model
1-P-25-0.5-1	0.5	63.5	compressive damage
1-P-25-0.5-2		57	compressive damage
1-P-25-1-3	1	82	shear damage
1-P-25-1-4		70	shear damage
1-P-25-1.5-5	1.5	87.5	shear damage
1-P-25-1.5-6		79.5	shear damage
1-P-25-2.5-7	2	89	shear damage
1-P-25-2.5-8		83	shear damage
1-P-25-4-9	4	76	shear damage
1-P-25-4-10		79	shear damage

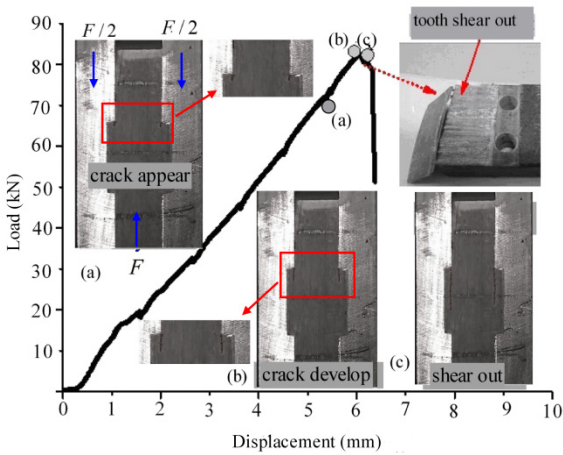


Fig. 9 Typical load–displacement curves and damage on specimen when depth of teeth is 2 mm

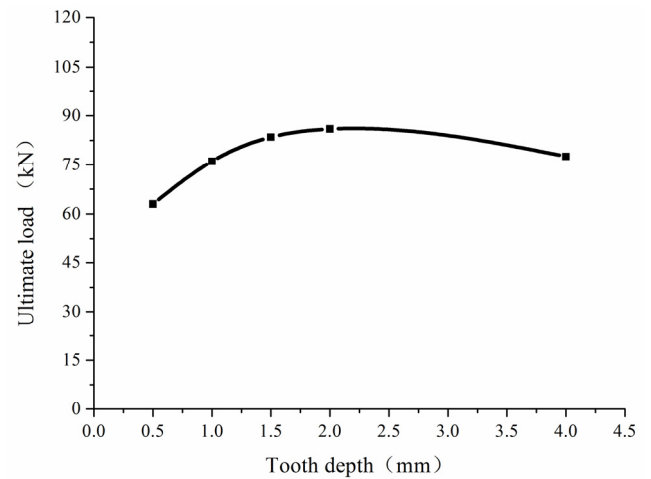


Fig. 10 Relationship between ultimate load and depth of teeth

4. Results and analysis

4.1 Influence of geometric parameters

There are two types of tooth damage because of the differences in the depth of teeth. (1) When the depth of teeth was 0.5 mm, compressive deformation was apparent at the composite tooth end, which resulted in local compressive damage (Fig. 8). During the initial loading phase, the measured displacement linearly correlated with the load as the load increased, and the appearance of the specimen did not markedly change. When the load increased to a specific value, the load–displacement curve tended to converge; the load slowly increased, while the displacement abruptly increased, and the plasticity was apparent (Fig. 8). (2) When the depth of teeth was high (1, 1.5, 2, and 4 mm), shear damage was apparent at the composite tooth end (Fig. 9). During the initial loading, the surface structure did not change, and no abnormal sounds were heard. As the load increased, subtle but continuous noise that was indicative of damage could be heard (Fig. 9(a)). Subtle horizontal cracks appeared at the front tooth root of the composite tooth and then quickly developed

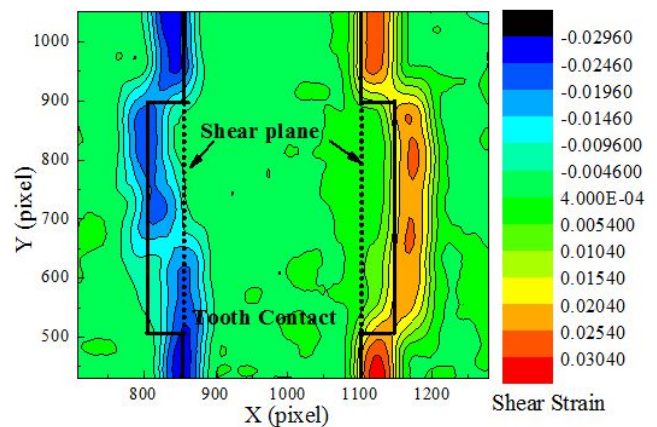


Fig. 11 Strain contour over joint

toward the rear (Fig. 9(b)). After the crack developed to a certain length, the tooth was damaged by the shear force, which was accompanied by a loud sound (Fig. 9(c)). The connection reached its ultimate bearing capacity. Before the load reached the bearing capacity, the relationship between

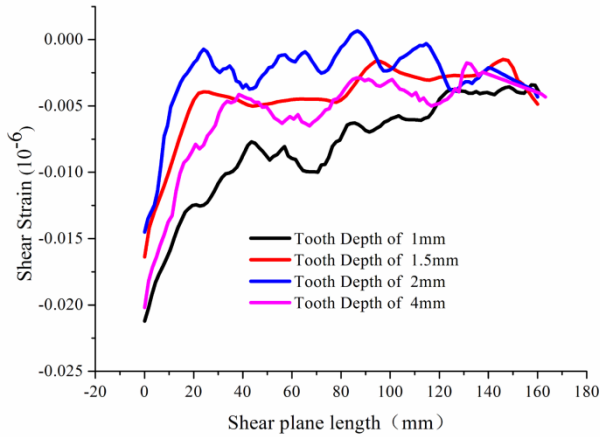


Fig. 12 Shear strain distribution on shear plane

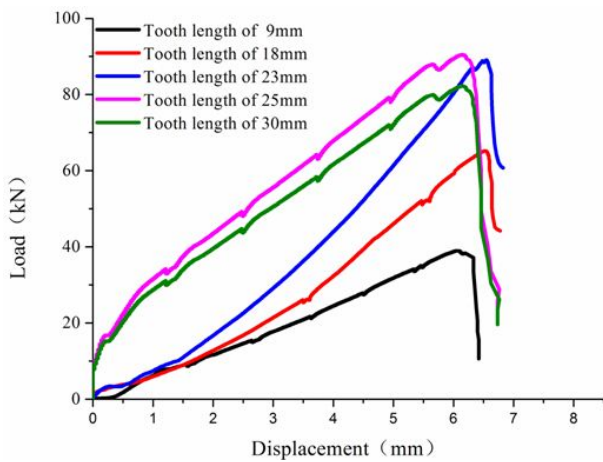


Fig. 13 Load-displacement curves for various lengths

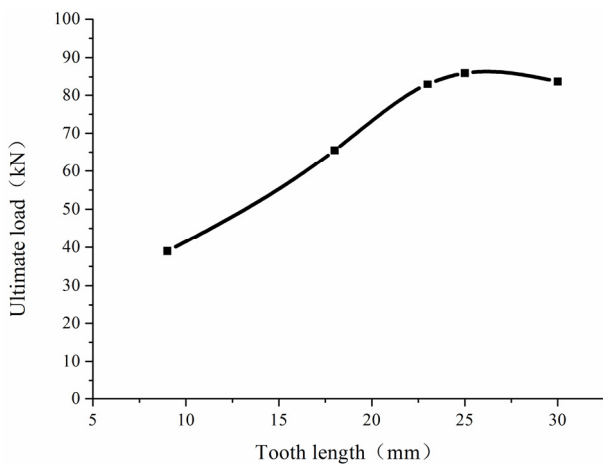


Fig. 14 Relationship between ultimate load and length

the load and the displacement increased monotonically. When the loading reached the bearing capacity, brittle damage occurred.

The relationship between the depth of teeth and ultimate load for the same pre-tightening force and length of teeth is shown in Fig. 10 and Table 4. When the depth of teeth was 1-2 mm, the ultimate load positively correlated with the

Table 5 Results for various lengths of teeth

Serial number	Tooth length (mm)	Ultimate load (kN)	Damage model
2-P-9-2-1	9	43	shear damage
2-P-9-2-2	9	35	shear damage
2-P-12-2-3	18	65	shear damage
2-P-12-2-4	18	66	shear damage
2-P-23-2-5	23	79	shear damage
2-P-23-2-6	23	87	shear damage
2-P-25-2-7	25	83	shear damage
2-P-25-2-8	25	89	shear damage
2-P-30-2-9	30	86.5	shear damage
2-P-30-2-10	30	81	shear damage

depth of teeth. When the depth increased from 2 mm to 4 mm, the ultimate load for a single tooth negatively correlated with the depth of teeth (Fig. 10). The strain contour over the joint obtained using the digital speckle is shown in Fig. 11 when the depth of teeth was 2 mm. The shear strain distribution on the shear plane obtained with the digital speckle is shown in Fig. 12 for the same load (the shear strain distribution is not discussed in this paper because no compressive damage was observed when the depth of teeth was 0.5 mm.) The figure shows that the maximal value of the strain negatively correlates with the depth of teeth when the depth of teeth is 1–2 mm. When the depth of teeth increases from 2 mm to 4 mm, the maximal value of strain negatively correlates with the depth of teeth. The maximal value of strain is the lowest when the depth of teeth is 2 mm. This conclusion is in agreement with the conclusion based on the theory of stress distribution: an optimal depth of teeth exists for a fixed composite plate thickness. The optimal depth of teeth can bear the maximum load (Deng *et al.* 2013).

The load-displacement curves for the different lengths of teeth are shown in Fig. 13. The relationships between the length of teeth and ultimate load for the same pre-tightening force and depth of teeth are shown in Fig. 14 and Table 5. The figure shows that the ultimate load of a single tooth positively correlates with the length of teeth during the initial stage of increasing the length. When the length

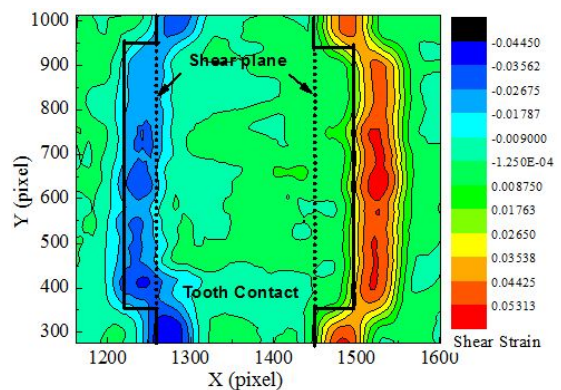


Fig. 15 Strain contour

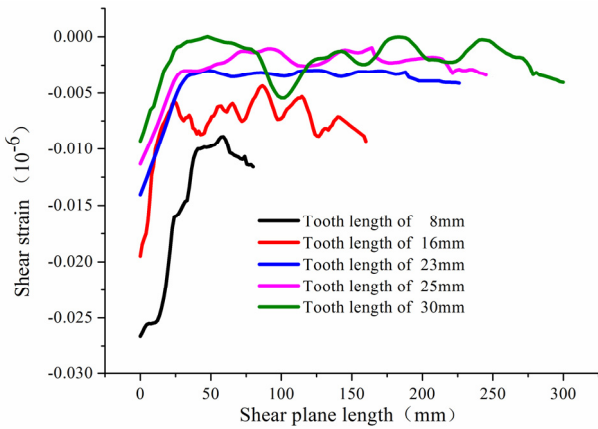


Fig. 16 Shear strain distribution on shear plane

Table 6 Results for various pre-tightening forces

Serial number	Pre-tight force (kN.m)	Ultimate load (kN)	Average ultimate load (kN)	Damage model
3-S-1-6-1	6	56	50	shear damage
3-S-1-6-2	6	44		shear damage
3-S-1-13-3	13	104	99.5	shear damage
3-S-1-13-4	13	95		shear damage
3-S-1-20-5	20	146	143	shear damage
3-S-1-20-6	20	140		shear damage
3-S-1-30-7	30	178	172.5	shear damage
3-S-1-30-8	30	167		shear damage
3-S-1-56-9	56	227	218	shear damage
3-S-1-56-10	56	209		shear damage

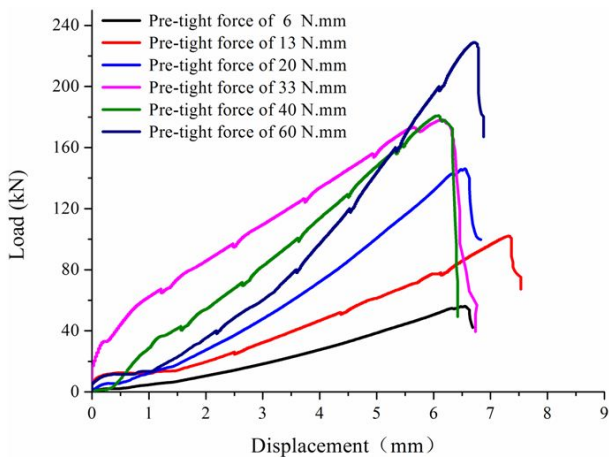


Fig. 17 Load–displacement curves for various pre-tightening forces

reached 23 mm, the bearing capacity of a single tooth was maximized and subsequently stabilized. The strain contour over the joint obtained with the digital speckle is shown in Fig. 15 for a tooth length of 30 mm. The shear strain distribution on the shear plane obtained with the digital

speckle is shown in Fig. 16 for different lengths of teeth and the same load. The figure shows that the stress concentrates at the end of the shear plane, and the shear strain on the shear plane is relatively large when the shear length is small. When the length of teeth increased, the strain at the end of the shear plane decreased. Furthermore, the bearing capacity of the joint increased. However, the shear strain was low along a certain length compared to the maximal shear strain when the length reached 30 mm. Furthermore, the bearing capacities of the 30 mm and 23 mm teeth were essentially identical. Hence, longer shear lengths are not necessarily preferable. Excessive shear lengths do not improve the load transfer capacity on the shear plane. Therefore, the influence of the shear length on the bearing capacity is moderate.

4.2 Influence of pre-tightening force

The load–displacement curves of the composite PTTCs are shown in Fig. 17 for different pre-tightening forces and when the depth of teeth was 2 mm. When the depth of teeth was 2 mm, the load–displacement curve of the composite tube PTTC agreed well with that of the composite plate PTTC. Before the load reached the ultimate value, the relationship between the load and displacement increased monotonically. When the load reached the ultimate value, brittle shear damage occurred. The change in the ultimate load of a single tooth as a function of the pre-tightening force is shown in Fig. 18 and Table 6. The ultimate load of the single tooth positively correlated with the pre-tightening force, the ultimate load increased with the pre-tightening force. Hence, higher pre-tightening forces are preferred.

4.3 Influence of number of teeth on ultimate bearing capacity of joint

The load–displacement curves of composite tube connections with varying number of teeth are shown in Fig. 19. This figure shows that the load–displacement curves of the composite tube PTTCs agree well with those of the composite plate PTTCs. Before the load reached the bearing capacity, the relationship between the load and displacement

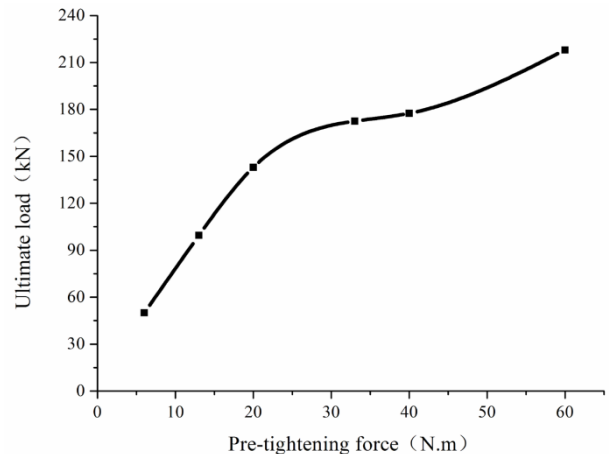


Fig. 18 Relationship between ultimate load and pre-tightening

Table 7 Results with different numbers of teeth

Serial number	Tooth number	Ultimate load (KN)	Average ultimate load (KN)	Damage model
4-S-1-56-1	1	227	218	shear damage
4-S-1-56-2		209		shear damage
4-S-3-56-3	3	428	436	shear damage
4-S-3-56-4		444		shear damage
4-S-5-56-5	5	531	545	shear damage
4-S-5-56-6		559		shear damage
4-S-7-56-7	7	718	727	shear damage
4-S-7-56-8		736		shear damage
4-S-8-56-9	8	745	758	shear damage
4-S-8-56-10		771		shear damage

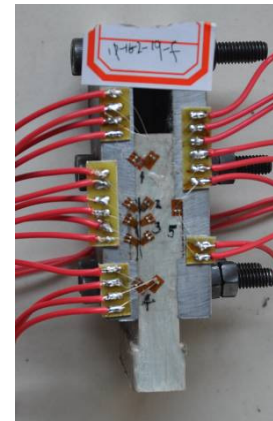


Fig. 21 First specimen

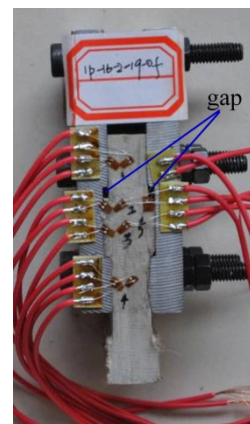


Fig. 22 Second specimen

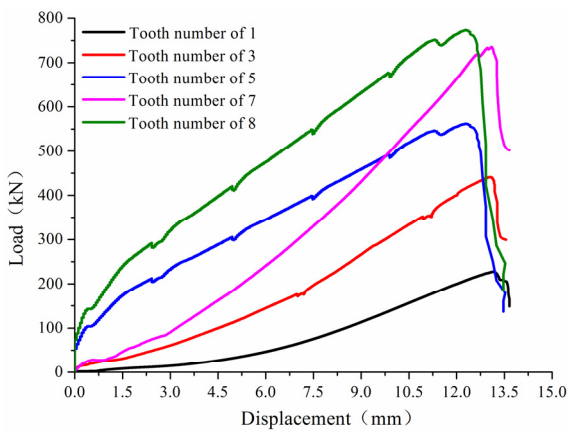


Fig. 19 Load–displacement curves for different numbers of teeth



Fig. 20 Damage on specimen

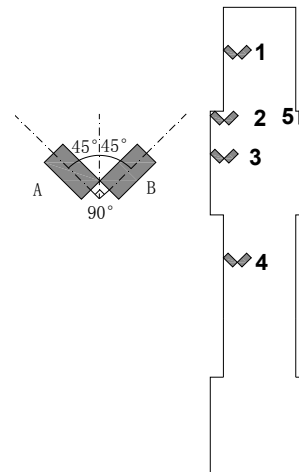


Fig. 23 Layout of strain gauges

increased monotonically. When the load reached the bearing capacity, brittle damage occurred. The main shear damage to the specimen is shown in Fig. 20. The values listed in Table 7 show that the bearing capacity improved threefold when the number of teeth increased from 1 to 7. However, the bearing capacity improved 1.04 times when the number of teeth increased from 7 to 8, and the bearing capacity

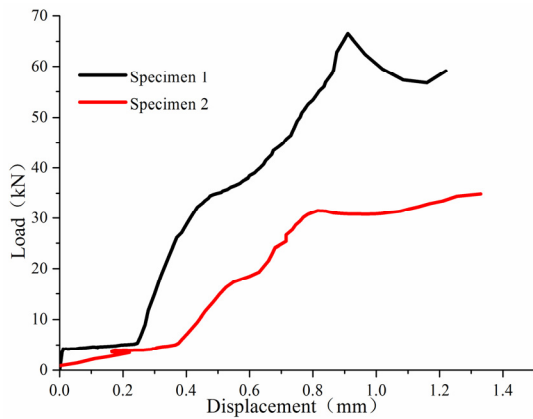
resulting from 7 teeth was equal to that of 8 teeth. When the number of teeth is low, the bearing capacity of the joint positively correlated with the number of teeth. When the number of teeth was increased to a given value, the bearing capacity of the joint stabilized because the composite was a brittle material, and the stress could not be redistributed. When the first tooth was broken, the entire joint lost its bearing capacity. The ultimate load of this joint was mainly

determined by the ultimate load of the first tooth.

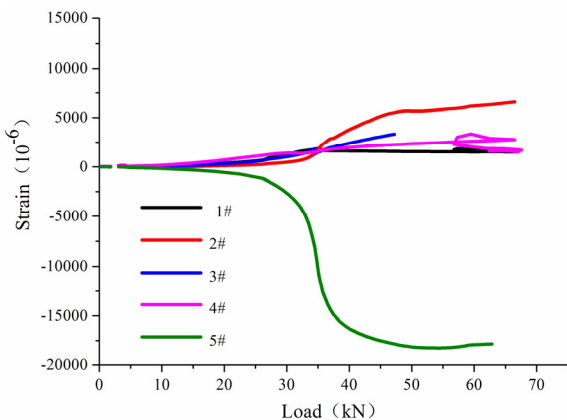
The composite connection efficiency can be defined as the ratio of the bearing capacity of the connecting location to the bearing capacity of the composite itself.

$$\eta = \frac{p_1}{p} \quad (1)$$

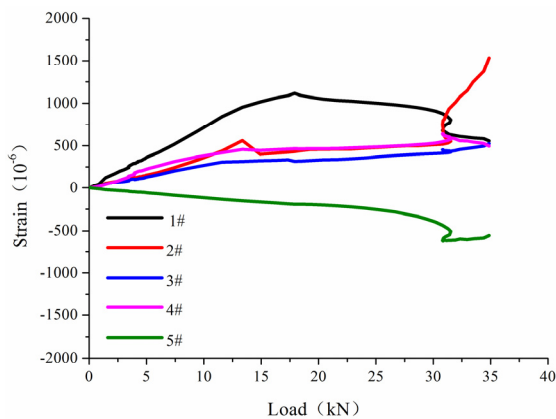
In this equation, p_1 is the ultimate load of the connecting location, and p is the ultimate load of the composite itself.



(a) Load–displacement curves of specimens



(b) Strain curve of specimen 1



(c) Strain curve of specimen 2

Fig. 24 Load–displacement curves and strain curves of specimens

In this study, a compression experiment on a composite tube PTTC was performed. Hence, p was the compressive bearing capacity of the composite. The compressive strength of the composite was 560 MPa; therefore, the compressive bearing capacity was 960 kN. According to Eq. (1), the new connection technique improves the compressive connection efficiency to 79% when eight teeth are used. Furthermore, the connection efficiency of this technology exceeds that of adhesive connections for the same thickness.

5. Force transfer mechanism

Research showed that the PTTC for composite tubes exhibited a relatively higher connection efficiency that could meet the demand of high-load composite components. Exerting a pre-tightening force on the joint not only improves the interlaminar shear strength, but also the resultant friction force on the interface between the composite and metal. The load is transferred by the interlaminar shear force and interface friction force. To research the effect of the interlaminar shear force and interface friction force, two specimens were tested in a compression experiment.

The first specimen was a normal single PTTC; the length was 16 mm, and the composite tooth matched well with the metal tooth (Fig. 21). In the second specimen, the length of the tooth space was 18 mm, with a 2 mm gap existing between the composite tooth and metal tooth (Fig. 22). This difference guaranteed that the end of the composite tooth could not transfer the load, which was only transferred by the friction force. A torque of 19 Nm was exerted. The bolts did not transfer the load during the load transfer process because the diameter of the bolt hole (10 mm) was larger than the diameter of the bolt (6 mm) (Fig. 22).

To understand the stress distribution on the composite during the loading process, strain gauges were installed on the two specimens. The layouts of these strain gauges are shown in Fig. 23. Rosettes were placed at positions 1, 2, 3, and 4 in order to measure the shear strain of the composite. The strain gauge at position 5 measured the compressive strain of the composite tooth end (Fig. 23).

The load–displacement and strain curves of the specimens at the measurement positions are shown in Fig. 24. This figure shows that the ultimate load of the second specimen was 30 kN, whereas the ultimate load of the first specimen was 68 kN. When the load was 30 kN, the load–displacement curve of the first specimen abruptly changed (Fig. 24(a)). This abrupt change indicated that the friction force primarily transferred the loads below 30 kN (Fig. 24(a)). When the load was 30 kN, the end of the composite tooth bore the compressive stress and began to transfer the load (Fig. 24(b)). The measured strain also points to this conclusion (Fig. 24(b)). The changes in the compressive strain were small at measurement position 5 for loads below 30 kN. The end of the tooth did not bear the compressive stress; only the friction force transferred the load (Fig. 24(a)). As the load increased, the compressive and shear strains increased rapidly at measurement positions 2, 3, and

5. However, the changes in the shear strains were small at measurement positions 1 and 4. This finding indicates that the friction force transferred the loads below 30 kN (Fig. 25(a)). When the load reached 30 kN, the end of the composite tooth bore the compressive stress and began to transfer the load (Fig. 25(b)). The friction force remained unchanged; the compressive force at the end of the tooth transferred the increased load. In the limit case, the friction force was approximately 30 kN. Hence, the bearing compressive force at the end of the tooth was 38 kN. Moreover, the interfacial shear force of the composite tooth transferred not only the 38 kN bearing compressive force, but also the friction force in the composite tooth (Fig. 25(c)). If the friction force in the composite tooth is 33% of the total friction force of the specimen, the interfacial shear force of the composite tooth bears a load of 48 kN, which is 70% of the bearing capacity of the specimen. This finding indicates that the interfacial shear force primarily transfers the external load in the limit case, and the bearing capacity of the joint depends on the capacity of the borne interfacial shear.

The interlaminar shear strength of a composite is generally determined by the property of the resin because of the unidirectional fiber layout. In fact, the shear strength is significantly higher than that of the pure resin. Research shows that the interlaminar shear strength of a composite is 2–3 times higher than the shear strength of the same pure epoxy resin template (Chen 2004). Moreover, the pre-tightening force can significantly improve the interlaminar shear strength of a composite material.

This relationship can be proven using several rules, e.g.,

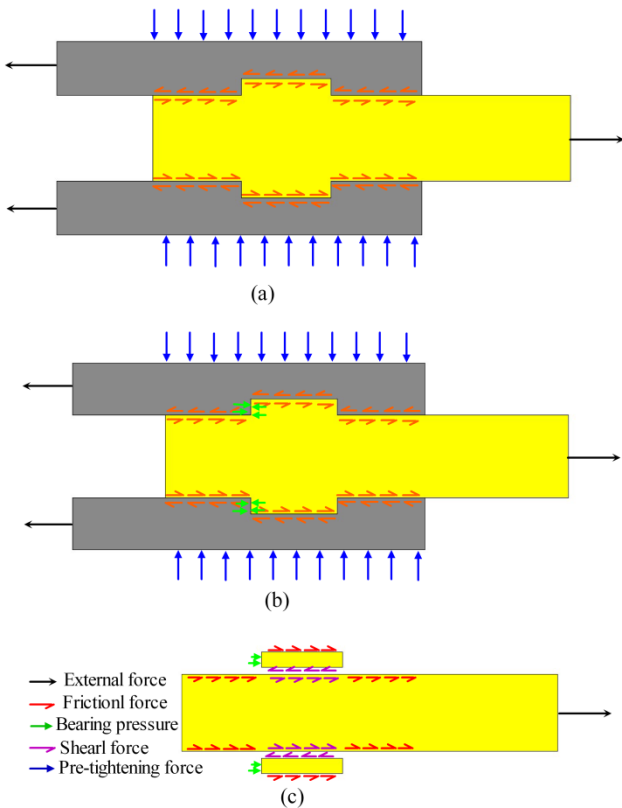


Fig. 25 Illustration of load transfer mechanisms

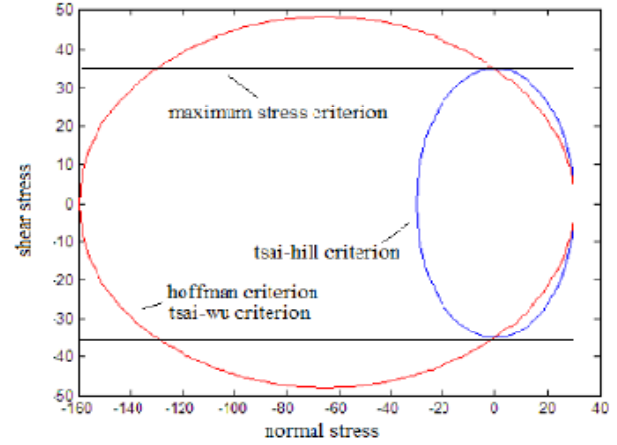


Fig. 26 Illustration of strength envelope

the Tsai–Hill criterion, Hoffman criterion, and Tsai–Wu tensor criterion. Under this stress state the expressions of the Hoffman criterion and Tsai–Wu tensor criterion are the same. These rules are expressed as follows:

Tsai–Hill criterion

$$\left(\frac{\sigma_2}{S_2}\right)^2 + \left(\frac{\tau_{12}}{S_{12}}\right)^2 = 1 \quad (2)$$

Hoffman criterion and Tsai–Wu tensor criterion

$$\left(\frac{1}{S_2^+} - \frac{1}{S_2^-}\right)\sigma_2 + \left(\frac{\sigma_2}{S_2^- S_2^+}\right)^2 + \left(\frac{\tau_{12}}{S_{12}}\right)^2 = 1 \quad (3)$$

Fig. 26 shows an illustration of the envelope for different strength rules and material strengths, where $S_2^+ = 30$ MPa, $S_2^- = 160$ MPa, and $S_{12} = 32$ MPa. The normal stress significantly influences the shear strength of the composite material. For the Hoffman criterion and Tsai–Wu tensor criterion, the compressive normal stress enhances the interlaminar shear strength of the composite within a certain range of normal stress, while the tensile normal stress reduces the interlaminar shear strength of the composite. Therefore, exerting a pretightening force on a composite can improve its shear strength.

6. Conclusions

The following conclusions can be reached based on the results of this study.

- In the experiments, the compressive connection efficiency reached 79% for the PTTC of a composite tube. For the same thickness, the bearing capacity was higher than that of an adhesive connection. Hence, the connection technique reported in this study provides a better mechanical performance for composite materials.
- The depth and length of teeth influence the damage mechanism and bearing capacity of the joint. When the depth of teeth is small, the compressive destruction at the composite tooth end is apparent.

When the depth is large, shear destruction is apparent. An optimal depth of teeth exists for a fixed composite thickness. The optimal depth of teeth can bear the maximum load. When the shear length is small, the bearing capacity of the joint positively correlates with the length of teeth. When the shear length is excessive, the load transfer capacity on the shear plane cannot be improved. Therefore, the shear length has a limited influence on the bearing capacity. When the number of teeth is low, the bearing capacity of the joint positively correlates with the number of teeth. When the number of teeth increases to a given value, the bearing capacity of the joint stabilizes.

- When the load is low, this is transferred by the friction force. When the load is large, the end of the composite tooth bears the compressive stress and begins to transfer the load, and the bearing capacity of the joint mainly depends on the interlaminar shear strength. Taking into account that the interlaminar shear strength of a pultruded composite is high and a pre-tightening force can significantly improve this strength, the proposed connection technology can be used to transfer higher loads.

Acknowledgments

The research described in this paper was financially supported by the National Science and Foundation Program of China under grant no. 11372355.

References

- Chen, X. (2004), Handbook of polymer matrix composite; Chemical Industry Press.
- Cheng, J.C. and Li, G. (2008), "Stress analyses of smart pipe joint integrated with piezoelectric composite layers under torsion loading", *Int. J. Solids Struct.*, **45**(6), 1153-1178.
- Das, R.R. and Pradhan, B. (2014), "Delamination damage analysis of laminated bonded tubular single lap joint made of fiber-reinforced polymer composite", *Int. J. Damage Mech.*, **23**(8), 772-790.
- Deng, A.Z., Zhao, Q.L., Li, F. and Chen, H. (2013), "Research on bearing capacity of single tooth to composite pre-tightened teeth connection", *J. Reinf. Plast. Comp.*, **32**(5), 1603-1613.
- Esmaili, F., Chakherlou, T.N. and Zehsaz, M. (2014), "Investigation of bolt clamping force on the fatigue life of double lap simple bolted and hybrid (bolted/bonded) joints via experimental and numerical analysis", *Eng. Fail. Anal.*, **45**(4), 406-420.
- Gamdania, F., Boukhilia, R. and Vadeana, A. (2015), "Tensile strength of open-hole, pin-loaded and multi-bolted single-lap joints in woven composite plates", *Mater. Des.*, **88**(5), 702-712.
- Girão Coelho, A.M. and Mottram, J.T. (2015), "A review of the behaviour and analysis of bolted connections and joints in pultruded fibre reinforced polymers", *Mater. Des.*, **74**(10), 86-107.
- Hosseinzadeh, R. and Taheri, F. (2009), "Non-linear investigation of overlap length effect on torsional capacity of tubular adhesively bonded joints", *Compos. Struct.*, **91**(8), 186-195.
- Huang, W., Fenu, L., Chen, B. and Briseghella, B. (2015), "Experimental study on K-joints of concrete-filled steel tubular truss structures", *J. Constr. Steel Res.*, **107**(2), 182-193.
- Ju, S., Jiang, D.Z., Sheno, R.A. and Xiao, J.Y. (2011), "Flexural properties of lightweight FRP composite truss structures", *J. Compos. Mater.*, **39**(5), 1921-1930.
- Karakuzu, R., Taylak, N., İçten, B.M. and Aktaş, M. (2008), "Effects of geometric parameters on failure behavior in laminated composite plates with two parallel pin-loaded holes", *Compos. Struct.*, **85**(1), 1-9.
- Kinloch, A.J. (1994), *Adhesion and Adhesives: Science and Technology*, (Reprinted), Chapman & Hall, London, UK.
- Li, G., Torres, S., Alaywan, W. and Abadie, C. (2005), "Experimental study of FRP tube-encased concrete columns", *J. Compos. Mater.*, **39**(2), 1131-1145.
- Li, F., Zhao, Q.L., Chen, H.S., Wang, J.Q. and Duan, J.H. (2010), "Prediction of tensile capacity based on cohesive zone model of bond anchorage for fiber-reinforced polymer tendon", *Compos. Struct.*, **92**(4), 2400-2405.
- Nemes, O., Lachaud, F. and Mojtabi, A. (2006), "A contribution to the study of cylindrical adhesive joining", *Int. J. Adhes. Adhes.*, **26**(2), 474-480.
- Oh, J.-H. (2007), "Nonlinear analysis of adhesively bonded tubular single-lap joints for composites in torsion", *Compos. Sci. Technol.*, **55**(8), 245-260.
- Prachasaree, W., Gangarao, H.V.S. and Shekar, V. (2009), "Performance evaluation of FRP bridge deck under shear loads", *J. Compos. Mater.*, **43**(3), 377-395.
- Rosales-Iriarte, F., Fellows, N.A. and Durodola, J.F. (2011), "Experimental evaluation of the effect of clamping force and hole clearance on carbon composites subjected to bearing versus bypass loading", *Compos Struct.*, **93**(7), 1096-1102.
- Scarselli, G., Castorini, E., Panella, F.W., Nobile, R. and Maffezzoli, A. (2015), "Structural behaviour modelling of bolted joints in composite laminates subjected to cyclic loading", *Aerosp. Sci. Technol.*, **53**(9), 213-221.
- Starikov, R. and Schön, J. (2001), "Quasi-static behavior of composite joints with protruding-head bolts", *Compos. Struct.*, **51**(4), 411-425.
- Ucsnik, S., Scheerer, M., Zarembo, S. and Pahr, D.H. (2010), "Experimental investigation of a novel hybrid metal-composite joining technology", *Compos. Part A*, **41**(6), 369-374.
- Wei, X. and Li, G. (2010), "Finite difference three-dimensional solution of stresses in adhesively bonded composite tubular joint subjected to torsion", *Int. J. Adhes. Adhes.*, **30**(7), 191-199.

CC